Growth and electronic structure of Cu on Cr_2O_3(0001)

2003 J. Phys.: Condens. Matter 15 1155

(http://iopscience.iop.org/0953-8984/15/8/301)

INSTITUTE OF PHYSICS PUBLISHING JOURNAL OF PHYSICS: CONDENSED MATTER

J. Phys.: Condens. Matter **15** (2003) 1155–1163 PII: S0953-8984(03)52969-1

Growth and electronic structure of Cu on Cr_2O_3(0001)

Wende Xiao, Kan Xie, Qinlin Guo[1] and E G Wang

State Key Laboratory for Surface Physics, Institute of Physics, Chinese Academy of Sciences, Beijing 100080, China

E-mail: qlguo@aphy.iphy.ac.cn

Received 3 September 2002, in final form 10 December 2002
Published 17 February 2003
Online at stacks.iop.org/JPhysCM/15/1155

Abstract

The deposition of Cu at room temperature on a Cr_2O_3(0001) substrate is studied by x-ray photoelectron spectroscopy, ultraviolet photoelectron spectroscopy and low-energy-electron diffraction. The results indicate that at RT Cu is highly dispersed on the substrate at initial deposition. X-ray induced Auger spectra, Auger parameter and ultraviolet photoelectron spectroscopy show that at the initial coverage the deposited Cu is in the Cu(I) state due to the interaction of Cu with the Cr_2O_3 substrate; Cu becomes metallic at Cu coverages of >4 monolayer equivalent. The formation of Cu two-dimensional or quasi-2D patches is followed by the formation of Cu three-dimensional clusters. Cu grows epitaxially on the Cr_2O_3(0001) films as Cu(111)R30° as observed by low-energy-electron diffraction.

1. Introduction

The metal–oxide interface is of extreme importance in many technological, for instance applications including microelectronic devices, oxide-supported transition-metal catalysts and metal-ceramic-based sensors. In recent years, considerable effort has been made to improve the understanding of the metal–oxide interface in regard to its physics and chemistry [1]. However, investigations at the interfaces of metals and bulk-single oxide crystals by electronic spectroscopies under ultrahigh vacuum (UHV) are often limited due to surface-charging problems and the difficulty of sample heating and cooling. To circumvent all these problems, ordered, thin metal oxide films supported on refractory metals, chosen to limit the lattice mismatch with the overlayer oxide, have been successfully prepared [2]. Of the oxides with the corundum structure, we have studied the deposition of Cu onto prepared V_2O_3(0001) films, and find that Cu grows epitaxially as Cu(111) [3].

[1] Author to whom any correspondence should be addressed.

0953-8984/03/081155+09$30.00

Chromium oxides are widely used materials as catalysts, anti-corrosive materials, etc. Although there are a few proposed phases of chromium oxide, the only stable bulk oxide is Cr_2O_3 with magnetic insulator properties. Studies on the structure and chemical reactivity of Cr_2O_3 surfaces have been carried out by preparing ordered oxide films on chromium single-crystal surfaces [4–12]. The growth and structure of chromium oxides have been investigated on Pt(111) [13, 14]. Oxides such as Cr_3O_4- and Cr_2O_3-like oxides have been prepared [13, 14]. Recently, the chromium oxides prepared on Cu(110) [15, 16], assuming a structure of CrO(111) at monolayer coverage and Cr_2O_3(111) at a coverage of more than two layers, have been reported. The growth of copper on polycrystalline and bulk-single crystal Cr_2O_3 at room temperature has been investigated [17, 18], and a week interaction of copper with the substrates is indicated.

In this paper, a Re(0001) surface with hexagonal structure has been selected as the substrate for growth of Cr_2O_3(0001) films, because its lattice constant (0.276 nm) is close to the in-plane O^{2-} sub-lattice (0.286 nm) in single crystal Cr_2O_3. The growth and interaction of copper deposited on these films were characterized using low-energy-electron diffraction (LEED), x-ray photoelectron spectroscopy (XPS) and ultraviolet photoelectron spectroscopy (UPS).

2. Experimental details

The experiments were carried out in an ESCALAB-5 system (VG Scientific Ltd) consisting of two UHV chambers. One of the chambers (the analysis chamber) was equipped with reverse view optics for LEED, dual-anode x-ray sources (Mg and Al), a He(I) source, and a hemispherical analyser for XPS and UPS. In the other chamber (preparation chamber), there was an Ar^+ sputtering gun, metal and gas sources and a sample heater. Both chambers had a base pressure of 2×10^{-9} mbar. The sample was prepared in the preparation chamber and analysed in the analysis chamber.

The Re(0001) sample (10 mm diameter disk with a thickness of 1.0 mm) was spot welded to a Mo holder with Ta slivers, allowing electron bombardment heating to 2500 K. A W–5% Re/W–26% Re thermocouple was spot welded close to the sample for temperature monitors. The surface was prepared by Ar^+ bombardment, followed by annealing in $\sim 10^{-7}$ mbar O_2 at about 1200 K with a subsequent flash to 2000 K in vacuum. After several treatments, no impurity was detected by XPS and a sharp hexagonal LEED pattern was observed.

The Cu doser consisted of a Cu wire wrapped tightly around a W filament. The chromium source was made from a chromium block (<3 mm in size) which was tightly wrapped with a W filament. The purity of the Cr and Cu sources was 99.9%. Before evaporation, the Cr and Cu sources were thoroughly degassed. The Cr_2O_3 film was grown on the Re(0001) by evaporation of Cr in 5×10^{-7} mbar O_2 ambience at about 700 K followed by about 900 K annealing in $\sim 10^{-7}$ mbar O_2 to enhance fully oxidation. Then the film was annealed by about 900 K without O_2 in vacuum for surface ordering. Cu deposition on Cr_2O_3 films with 15–20 monolayer equivalent (MLE) thickness of Cr on the substrate was carried out at RT. The deposition rates of Cr and Cu were about 0.4 and 0.3 ML min^{-1}, respectively, calibrated via XPS of Cr 2p and Cu 2p deposited onto the Re(0001) surface as a function of deposition time. Since Cu is not necessarily grown on Cr_2O_3 film layer-by-layer, we prefer to use the MLE as a measurement for Cu coverage.

The XPS analyses were performed using a Mg Kα x-ray source (1253.6 eV) and a pass energy of 50 eV was used while collecting all data. Binding energies (BEs) were calibrated with respect to the Au $4f_{7/2}$ (BE = 84.0 eV) and Cu $2p_{3/2}$ (BE = 932.7 eV) features of metallic Au and Cu, respectively. Helium of 99.999% purity was used for He(I) UPS (21.2 eV). All data were recorded at RT.

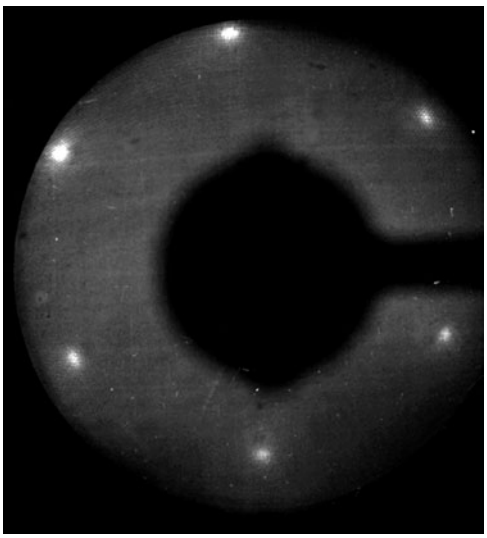

Figure 1. LEED pattern from a 20 MLE Cr_2O_3(0001) film on the Re(0001) substrate. $Ep = 26$ eV.

3. Results and discussion

3.1. Preparation of Cr_2O_3(0001) films

Prior to film preparation, several Ar^+ bombardment and annealing cycles at high temperature were carried out, and the sharp hexagonal LEED pattern of the clean Re(0001) surface was observed. Figure 1 demonstrates a hexagonal LEED pattern after a ∼20 MLE chromium oxide film is grown on the Re(0001) surface. On this surface, no Re signal was detected by XPS. Due to the variable valence of chromium, several compounds may form in the chromium–oxygen system with different structures and stoichiometries, such as CrO, CrO_2, Cr_2O_3 and Cr_3O_4. Among them three kinds of chromium oxide surfaces with hexagonal symmetry exist, i.e. CrO(111), Cr_3O_4(111) and Cr_2O_3(0001). Maetaki *et al* [15, 16] have found that the hexagonal LEED pattern from a CrO(111) film on a Cu(110) surface exists at the chromium oxide coverage up to ∼1.0 MLE. Zhang *et al* [13, 14] observed a Cr_3O_4(111) film on Pt(111) up to around 2.0 MLE coverage, and after annealing at a temperature higher than 700 K it was changed into Cr_2O_3(0001) [13–16]. At higher coverage, Cr_2O_3(0001) formed [13–16]. Since Cr_2O_3 is the only stable chromium oxide bulk phase, and considering our chromium oxide film with about 20 MLE thickness was annealed at about 900 K in vacuum, the prepared chromium oxide is very likely to be Cr_2O_3(0001).

To confirm the formation of Cr_2O_3(0001) film, further experiments have been carried out. It is known that x-ray core level photoemission is very sensitive to the chemical environment of atoms. Various chromium oxides can be distinguished from each other by XPS. Previous studies have shown that the BEs of Cr $2p_{3/2}$ are 576.0 and 576.9 eV for CrO(111) and Cr_2O_3(0001) [15, 16], respectively. Cr_3O_4(111) contains two kinds of Cr cations, Cr^{2+} and Cr^{3+}, so the XPS spectrum shows broader and asymmetric peaks compared with that of CrO(111) or Cr_2O_3(0001), and can be fitted with two peaks assigned to Cr^{2+} and Cr^{3+} [13, 14]. XPS data for our chromium oxide film with 20 MLE thickness are shown in figure 2. Since the BE of Cr $2p_{3/2}$ is 576.7 eV, the Cr $2p_{3/2}$–Cr $2p_{1/2}$ BE separation is 9.8 eV, and O 1s is 530.2 eV (not shown), these values are consistent with former XPS studies on single-crystal

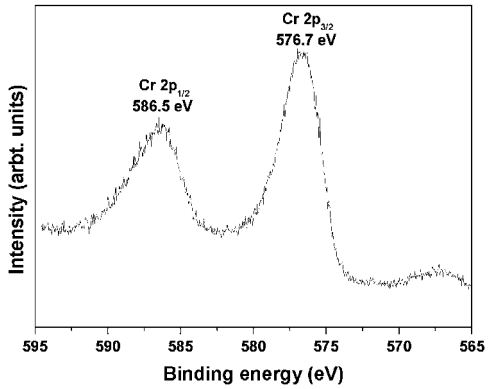

Figure 2. XPS of Cr_2O_3 film with thickness 20 MLE on a Re(0001) substrate. Mg Kα, $h\nu = 1253.6$ eV.

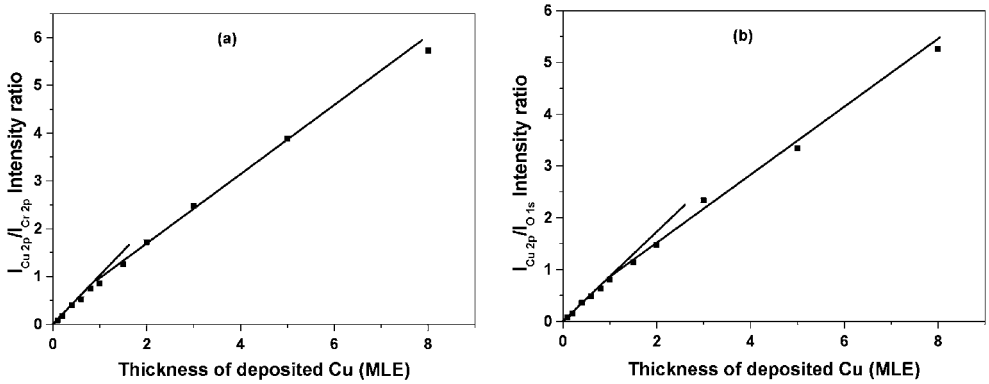

Figure 3. The XPS intensity ratio $I_{Cu\,2p}/I_{Cr\,2p}$ (a) and $I_{Cu\,2p}/I_{O\,1s}$ (b) as a function of Cu deposition at RT.

samples of Cr_2O_3 [19], power samples of Cr_2O_3 [20–22], and Cr_2O_3 overlayers formed on Cr(110) [8, 9, 12], Pt(111) [13, 14], and Cu(110) surfaces [15, 16]. It is therefore concluded that the chromium oxide film we prepared is $Cr_2O_3(0001)$.

3.2. Growth of Cu on the Cr_2O_3(0001) films

Cu deposition was carried out step by step on the $Cr_2O_3(0001)$ film at RT and the XPS spectra were recorded after each deposition. Since XPS is a surface sensitive technique and gives information on the composition and the chemical state in the range of 1–4 nm, it is normally widely used as a quantitative tool to investigate the growth of adatoms on substrates. Figure 3 shows the XPS intensity ratio of the Cu $2p_{3/2}$ peak to the Cr $2p_{3/2}$ peak (figure 3(a)) and the Cu $2p_{3/2}$ peak to the O 1s peak (figure 3(b)) versus the Cu coverage in MLE. Each curve can be well fitted by a simple model with two linear segments. Their slopes are changed with increasing Cu deposition. This suggests two different types of growth mode. At submonolayer coverage, the deposited Cu is highly dispersed, most possibly forming two-dimensional (2D) patches or quasi-2D patches, resulting in a rapid increase in XPS signal. Above 1 MLE coverage of Cu, three-dimensional (3D) clusters form. At this region, the XPS intensity of Cu

is increased slowly, as seen in figure 3. This growth mode is similar to what we have found for Cu growth on bulk single crystal Cr_2O_3(0001) surfaces [18], but different from the layer-by-layer mode of Cu deposited on a polycrystalline Cr_2O_3 surface at RT [17]. We notice that signal of Cr and O can still be detected by XPS even after about 20 MLE Cu deposition. This means that at this coverage the substrate still has naked exposed areas because of formation of 3D clusters of Cu. Since no Cu superstructure can be observed by LEED until the growth for at least 15 MLE Cu deposition, based on the application of incident energy having a coherence length of about 10 nm, at lower coverage the Cu clusters are smaller. We also notice that the XPS intensity ratio of the Cr $2p_{3/2}$ peak to the O 1s peak stays basically constant, which suggests no Cu atom diffuses into the Cr_2O_3(0001) substrate.

Generally, the growth behaviour of an overlayer on a substrate is related to the surface free energy of the overlayer (γ_0), the surface free energy of the substrate (γ_s), and the interfacial energy between them (γ_i). If $\gamma_s > \gamma_0 + \gamma_i$, the overlayer will begin to grow by covering the substrate with a continuous layer, via the FM (Frank–Van der Merwe, layer-by-layer) or the SK (Stranski–Krastanov, layer-plus-island) growth mode. If $\gamma_s < \gamma_0 + \gamma_i$, the overlayers are likely to grow in 3D clusters (the VW, Volmer–Weber island, growth mode).

In our present paper, the surface free energy of Cu(111) (1.8 J m^{-2}) is significantly lower than that of Cr_2O_3(0001) (for a relaxed surface, the surface free energy of Cr_2O_3(0001) is 3 J m^{-2} [23], and for an unrelaxed one it is much higher) [24, 25]. A Cu–O bond can form between a Cu overlayer and a Cr_2O_3 substrate (see section 3.3). This indicates that Cu is thermodynamically favoured to form a complete monolayer. However, as we will see in section 3.3, after the Cu deposition of 0.4 MLE, the surface of the substrate is saturated with Cu_2O, which has a much lower surface free energy. The further deposited Cu is inclined to form 3D clusters, following 3D mode growth.

A clear LEED pattern of a Cu(111)R30° superstructure on a Cr_2O_3(0001) film with a thickness of about 20 MLE is shown in figure 4. This is similar to the previous results of Cu on the oxides with corundum structure, such as Cu on Al_2O_3(0001) [26], V_2O_3(0001) [3], and bulk single crystal Cr_2O_3(0001) [18]. Using the lattice constant of bulk Cr_2O_3 (assuming the lattice constant of the prepared Cr_2O_3(0001) film is 0.5 nm, a value of bulk Cr_2O_3), we calculate the distance between Cu atoms ($a^* = b^* = 2/\sqrt{3}a_0$, where a^* and b^* are reciprocal lattice vectors and a_0 is the lattice constant) in Cu(111) to be 0.26 nm, which agrees well with the bulk 0.256 nm Cu value.

3.3. Interaction of Cu with Cr_2O_3(0001) substrates

Previous XPS studies have shown that one major difference between Cu_2O and CuO is the prominent satellite structure on the high BE side of the Cu 2p core lines [27, 28]. For the Cu and the Cu_2O, the peak shapes of Cu 2p are similar and the BE values are very close (for Cu(0) the BE value of Cu $2p_{3/2}$ is 932.7 eV and for Cu(I) it is 932.6 eV) [28, 29]. It is therefore difficult to further distinguish between Cu(0) and Cu(I) on the basis of the energy shift of Cu core level alone, but it can be achieved by considering the corresponding x-ray induced Auger Cu(LMM) spectra and the BE, i.e. Auger parameter α (the sum of the kinetic energy of the x-ray induced Auger peak and the BE value of the highest photoemission peak, i.e. Cu $2p_{3/2}$) [29]. Figure 5 shows the XPS spectra of Cu $2p_{1/2}$ and $2p_{3/2}$ spin–orbit doublet with increasing deposition of Cu on the Cr_2O_3(0001) film. The peaks marked a and b are induced by Mg $K\alpha_{3,4}$. Since no shake-up satellite line is observed for both 2p lines, the chemical state of Cu should not be Cu(II). X-ray induced Auger Cu(LMM) spectra are also studied (not shown). At low coverages, the Cu(LMM) signal is found at 914.6 eV kinetic energy in line with literature data for Cu_2O [29]. This line steadily shifts to higher kinetic

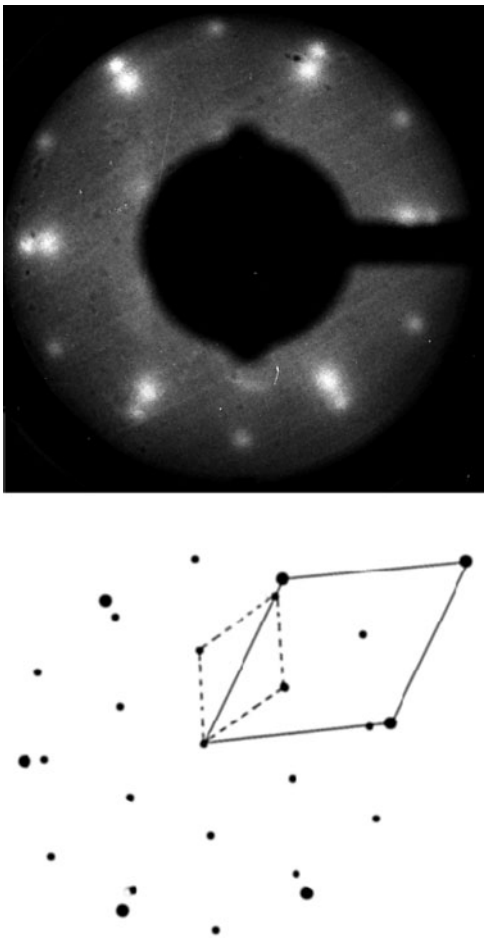

Figure 4. Top, LEED pattern from epitaxial copper superstructure, Cu(111)/Cr_2O_3(0001)/Re(0001). $Ep = 60$ eV. The respective unit cells are indicated in the bottom. The large (full line) unit cell corresponds to Cu(111) and the small (broken line) unit cell to the Cr_2O_3(0001) surface.

energy with increasing Cu deposition, finally reaching the value of 918.6 eV for metallic Cu [29]. The changes of the Auger parameter α as a function of Cu coverage is shown in figure 6. It can be seen that there is a gradual approach α from the Cu(I) value of 1847.3 eV to the metallic Cu value of 1851.3 eV [29]. Figure 6 indicates the existence of the Cu(I) state at the beginning of Cu growth on chromium oxide films. Similar results have been found for Cu on Fe_2O_3 [30, 31], Al_2O_3 [26, 32, 33], V_2O_3 [3], and bulk single crystal Cr_2O_3(0001) surfaces [18]. Maetaki *et al* [15, 16] have reported the formation of Cu^+-oxide at the surface of chromium oxide/Cu(110), but they have heated the surface with an oxygen ambient. In our experiments, the Cu deposition was carried out in vacuum without oxygen, so the Cu(I) chemical state must origin from the charge transfer from Cu to the Cr_2O_3 substrate. We note that the value of 1847.3 eV is much lower than the Cu_2O value of 1848.7 eV [29], hence the Cu(I) may form at the defects in the substrate surface and the Cu–O bond is stronger than that of bulk Cu_2O. At a coverage of 4–5 MLE, Cu becomes metallic. This suggests that only the initial deposition of Cu interacts with the substrate.

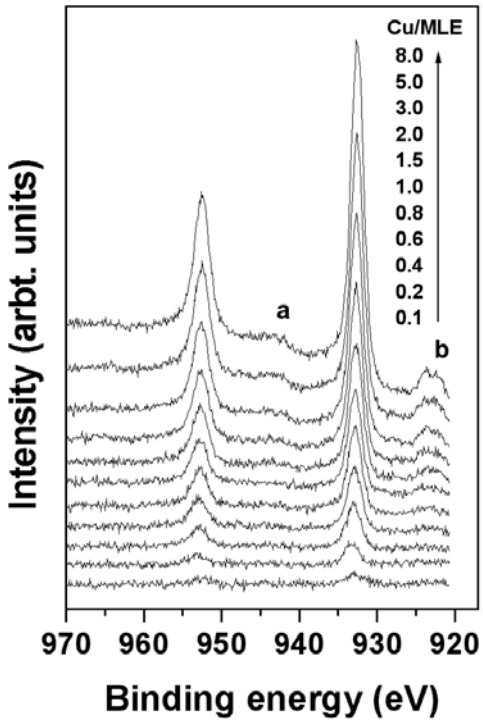

Figure 5. XPS of deposited Cu as a function of coverage. Mg Kα, $h\nu = 1253.6$ eV.

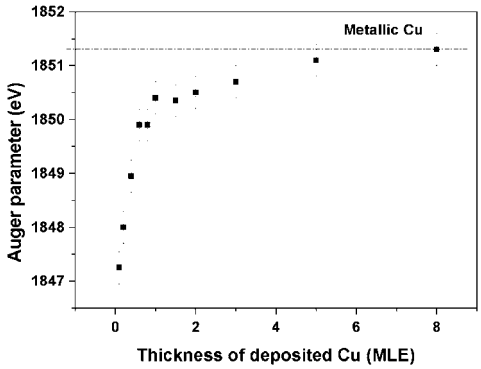

Figure 6. Auger parameter changes with increasing Cu on the Cr_2O_3(0001) surface.

Further information about interaction between Cu and Cr_2O_3 has been obtained from He(I) UPS. Figure 7 shows He(I) UP spectra for a Cr_2O_3(0001) surface with increasing Cu deposition. For clean Cr_2O_3(0001), the peak located at 2.5 eV below the Fermi level is attributed to localized 3d states, and two other peaks located at 4.9 and 6.7 eV, respectively, below Fermi level are assigned to the O(2p) orbital and to the Cr–O hybridization, comparable with previous UPS and XPS valence band studies [8, 16–19, 34–40]. After 0.4 MLE Cu deposition, the maximum shift, 0.6 eV to higher BE, the similar position of energy for the Cu(I) state [18, 32, 33, 41–43], is observed. This position of energy is higher than that of

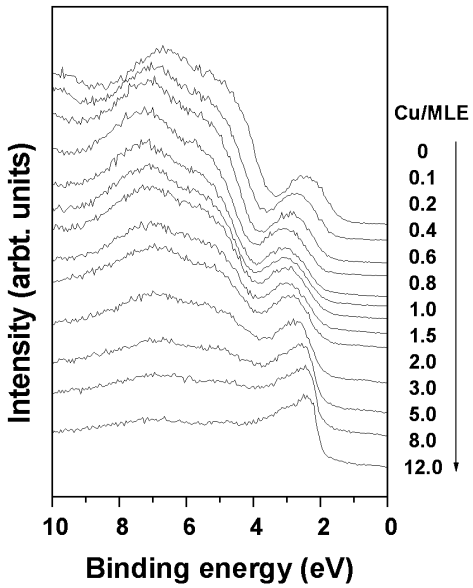

Figure 7. He(I) UP spectra as a function of Cu coverage on Cr_2O_3(0001)/Re(0001).

metallic Cu (2.5 eV) [18, 32, 33, 41, 42], and it shifts to low energies with further Cu deposition approaching the bulk Cu characteristic, as shown in figure 7. This strongly suggests that Cu(I) exists at initial coverage. At higher coverage, Cu atoms agglomerate into 3D clusters and gradually show metallic features, being consistent with former discussion.

4. Conclusions

A study of the growth and electronic structure of Cu on ordered Cr_2O_3(0001) films is performed using LEED, XPS and UPS. The results indicate that at RT Cu is highly dispersed on the substrate at initial deposition, and Cu(I) state derived features have been observed. At Cu coverages of >4 MLE, Cu becomes metallic. The formation of Cu 2D or quasi-2D patches is followed by the formation of Cu 3D clusters. A Cu(111)R30° superstructure on a Cr_2O_3(0001) surface has been observed by LEED.

Acknowledgments

The financial support of the Natural Science Foundation of China (grant numbers 10074079, 19974069 and 19874077) and the State Key Project of Fundamental Research (G1998061310 and G2000067103) are gratefully acknowledged.

References

[1] Campbell C T 1997 *Surf. Sci. Rep.* **27** 1
[2] Street S C, Xu C and Goodman D W 1997 *Annu. Rev. Phys. Chem.* **48** 43
[3] Xiao W, Xie K, Guo Q and Wang E G 2002 *J. Phys. Chem.* B **106** 4721
[4] Kennett H M and Lee A E 1972 *Surf. Sci.* **33** 377
[5] Ekelund S and Leygraf C 1973 *Surf. Sci.* **40** 179

[6] Watari F and Cowley J M 1981 *Surf. Sci.* **105** 240
[7] Brown N M D and You H 1990 *Surf. Sci.* **233** 317
[8] Ma H, Berthier Y and Marcus P 1999 *Appl. Surf. Sci.* **153** 40
[9] Xu C, Hassel M, Kuhlenbeck H and Freund H J 1991 *Surf. Sci.* **258** 23
[10] Bender M, Ehrlich D, Yakovkin I N, Rohr F, Bäumer M, Kuhlenbeck H, Freund H J and Staemmler V 1995 *J. Phys.: Condens. Matter* **7** 5289
[11] Stierle A, Koll T and Zabel H 1998 *Phys. Rev.* B **58** 5062
[12] Maurice V, Cadot S and Marcus P 2000 *Surf. Sci.* **458** 195
[13] Zhang L, Kuhn M and Diebold U 1997 *Surf. Sci.* **375** 1
[14] Zhang L, Kuhn M and Diebold U 1997 *J. Vac. Sci. Technol.* A **15** 1576
[15] Maetaki A and Kishi K 1998 *Surf. Sci.* **411** 35
[16] Maetaki A, Yamamoto M, Matsumoto H and Kishi K 2000 *Surf. Sci.* **445** 80
[17] Castro V D, Furlani C, Polzonetti G and Cozza C 1988 *J. Electron Spectrosc. Relat. Phenom.* **48** 297
[18] Guo Q, Gui L, Møller P J and Binau K 1996 *Appl. Surf. Sci.* **92** 513
[19] Werfel F and Brümmer O 1983 *Phys. Scr.* **28** 92
[20] Howng W Y and Thorn R J 1980 *J. Phys. Chem. Solids* **41** 75
[21] Carver J C, Schweitzer G K and Carlson T A 1972 *J. Chem. Phys.* **57** 973
[22] Ikemoto I, Ishii K, Kinoshita S, Kuroda H, Franco M A A and Thomas J M 1976 *J. Solid State Chem.* **17** 425
[23] Vitos L, Ruban A V, Skriver H L and Kollar J 1998 *Surf. Sci.* **411** 186
[24] Rehbein C, Harrison N M and Wander A 1996 *Phys. Rev.* B **54** 14066
[25] Rowley A J, Wilson M and Madden P A 1999 *J. Phys.: Condens. Matter* **11** 1903
[26] Møller P J and Guo Q 1991 *Thin Solid Films* **201** 267
[27] Yin L, Adler I, Tsang T, Matienzo L J and Grim S O 1974 *Chem. Phys. Lett.* **24** 81
[28] Mcintyre N S and Cook M G 1975 *Ann. Chem.* **47** 2208
[29] Wagner C D, Riggs W M, Moulder L E and Muilenberg G E 1979 *Handbook of X-ray Photoelectron Spectroscopy* (USA: Perkin-Elemer Corporation Physical Electronics Division)
[30] Guo Q and Møller P J 1995 *Surf. Sci.* **340** L999
[31] Møller P J, Guo Q and Gui L 1996 *Thin Solid Films* **281/282** 76
[32] Guo Q and Møller P J 1991 *Surf. Sci.* **244** 228
[33] Guo Q and Møller P J 1990 *Vacuum* **41** 1114
[34] Wertheim G K, Guggenheim H J and Hüfner S 1973 *Phys. Rev. Lett.* **30** 1050
[35] Eastman D E and Freeout J L 1975 *Phys. Rev. Lett.* **34** 395
[36] Beatham N, Orchard A F and Thornton G 1981 *J. Phys. Chem. Solids* **42** 1051
[37] Gewinner G, Peruchetti J C, Jaegle A and Kalt A 1978 *Surf. Sci.* **78** 439
[38] Sakisaka Y, Kato H and Onchi M 1982 *Surf. Sci.* **120** 150
[39] Kirby R E, Garwin E L, King F K and Nyaiesh A R 1987 *J. Appl. Phys.* **62** 1400
[40] Moffat T P and Latanision R M 1992 *J. Electrochem. Soc.* **139** 1869
[41] Ohuchi F S, French R H and Kasowski R V 1987 *J. Appl. Phys.* **62** 2286
[42] Ohuchi F S, French R H and Kasowski R V 1987 *J. Vac. Sci. Technol.* A **5** 1175
[43] Benndorf C, Caus H, Egert B, Seidel H and Thieme F 1980 *J. Electron Spectrosc. Relat. Phenom.* **19** 77